2014 IEEE International Conference on Robotics & Automation (ICRA)
Hong Kong Convention and Exhibition Center
May 31 - June 7, 2014. Hong Kong, China

Collision-Free Guidance Control for Multiple Small Helicopters

Yoshihiko Aida[1], Satoshi Suzuki[2], Yohei Fujisawa[1], Kojiro Iizuka[2], Takashi Kawamura[2] and Yuichi Ikeda[3]

Abstract— **In this study, we aim at realizing autonomous simultaneous flight of multiple small helicopters. In such situation, collision avoidance of the helicopters should be considered in guidance control system to improve safety and reliability of the flight system. In this paper, we construct a collision-free guidance control system for multiple small helicopters. The collision avoidance problem is regarded as a control problem with state restrictions, and the theory of Nonlinear Model Predictive Control (NMPC) is applied to the guidance control system. A simple nonlinear guidance model is used for design of NMPC to reduce the computational cost. A novel position constraint is proposed for optimizing the avoidance trajectory of each helicopter. The effectiveness of the designed control system and proposed constraints are verified by numerical simulation and flight experiment.**

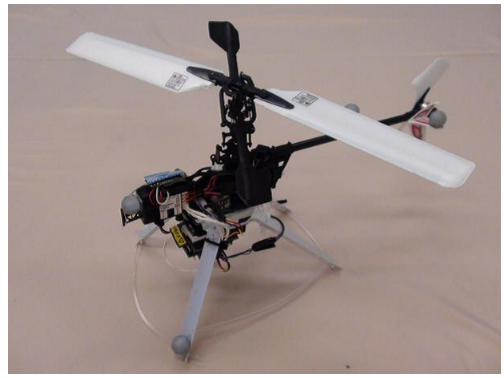

Fig. 1. Overview of small helicopter

I. INTRODUCTION

In the last decade, unmanned aerial vehicle (UAV) technology has drastically improved, and UAVs are now used not only in research and development but also for various practical purposes. UAVs are safer and more convenient than manned aircraft and they can potentially have a wide range of applications. Therefore, several researchers have focused on development, operation, and autonomous control of various types of UAVs [1]-[10]. In such UAVs, we are especially interesting in small unmanned helicopter.

Recently, small unmanned helicopter weighing less than 5 kg have attracted considerable attention owing to their ease of handling [11]. However, the abilities of such small helicopter are strictly limited, for example small payload capability and short flight endurance. Moreover, small helicopters may fail frequently as a result of their limited sensing and computational payload. To overcome the problem, the simultaneous flight of multiple small unmanned helicopters has been studied [12][13]. The main advantage of simultaneous flight is efficiency and fault tolerance capability. Operating efficiency may drastically increase when the multiple helicopters share their task, thus the loss by the limited flight endurance of individual helicopter could be complemented. Additionally, even one helicopter has fallen into troubles, the task could be accomplished by other helicopters. Therefore robustness and fault tolerance capability of the entire system may improve.

In the simultaneous flight, a collision of each helicopter is major problem, and it should be considered in the design of a guidance system. Several approaches for collision avoidance of multiple mobile robots have already been proposed. For example, potential field method [16] is the most popular method for collision-free guidance because it could be easily implemented. However, it is well known that these methods are prone to local minima. Model Predictive Control (MPC) is another solution to realize the collision avoidance, and has been adopted for a lot of studies [12]-[15]. However, MPC used in these researches is computationally expensive, thus it needs large-scale device for calculation. Moreover, trajectory in avoidance behavior has not been optimized. Therefore, undesirable trajectory may be generated at the time of collision avoidance.

In this study, Nonlinear Model Predictive Control (NMPC) is adopted for collision-free guidance control of multiple small helicopters. A simple nonlinear guidance model is used for design of NMPC to reduce the computational cost. A novel position constraint is proposed for optimizing the avoidance trajectory of each helicopter. The rest of this paper is organized as follows. Control system design for collision-free guidance control is presented in Section II. We propose double feedback loop system realizing the attitude and guidance control individually, and NMPC is applied for guidance control system. Numerical simulation and experiment are performed in Section III and section IV to verify the designed guidance control system. Finally, conclusion of this work is shown in section V.

II. CONTROL SYSTEM DESIGN

In this section, the collision-free guidance control system for small helicopter is designed. The overview of a small helicopter used in this study is shown in Fig.1. Figure. 2 shows the overview of proposed control system. A hierarchical control structure is adopted for reducing the compu-

*This work was partly supported by JSPS KAKENHI Grant Number 24760185

[1]Y. Aida and Y. Fujisawa are with the Graduate School of Science and Technology, Shinshu University, Nagano, Japan s-s-2208 at shinshu-u.ac.jp

[2]S. Suzuki, K. Iizuka and T. Kawamura are with the Faculty of Textile Science and Technology, Shinshu University, Nagano, Japan

[3]Y. Ikeda is with the Faculty of Engineering, Shinshu University, Nagano, Japan

978-1-4799-3684-7/14/$31.00 ©2014 IEEE

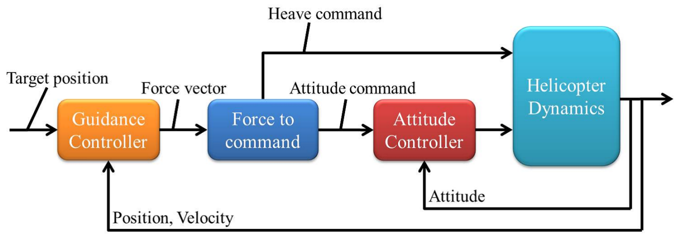

Fig. 2. Overview of entire control system

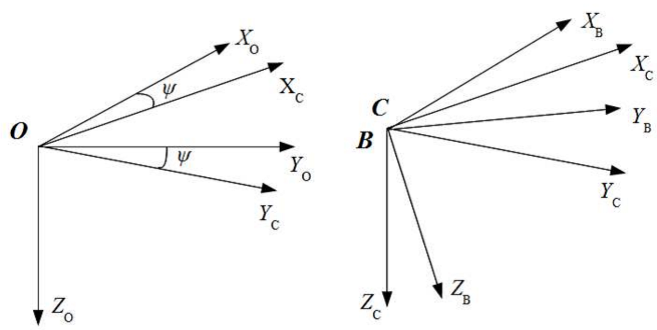

Fig. 3. Coordinate system

tational cost. The control system consists of two feedback control loop, attitude control loop (inner loop) and guidance control loop (outer loop). The attitude controller stabilizes the attitude dynamics of the helicopter and makes the attitude follows desired attitude. The guidance controller generates appropriate desired attitude and desired rotor thrust to realize desired external force vector that is needed to guide the helicopter to target position. NMPC is adopted only for the guidance controller; therefore, number of states which are dealt with in NMPC could decrease and the computational cost for NMPC could also be reduced than which of full-state feedback case.

A. Coordinate Systems

First, coordinate systems used for control system design are defined. $\boldsymbol{O}$-frame denotes the inertial frame; its origin is fixed at arbitrary point on the ground. $\boldsymbol{Z}_O$ is aligned with the direction of gravity. $\boldsymbol{B}$-frame denotes the body frame; its origin is fixed at the centre of gravity of the helicopter. $\boldsymbol{X}_B$ is aligned with the forward direction of the body, $\boldsymbol{Y}_B$ with rightward direction, and $\boldsymbol{Z}_B$ with downward direction. Besides, the attitude of the helicopter is defined as the attitude of $\boldsymbol{B}$-frame relative to $\boldsymbol{O}$-frame, and Roll-Pitch-Yaw angle ϕ, θ, ψ are used for attitude expression. Additionally, $\boldsymbol{C}$-frame denotes the reference frame; its origin is same as the origin of $\boldsymbol{B}$-frame. $\boldsymbol{X}_C$-$\boldsymbol{Y}_C$ plane is parallel with $\boldsymbol{X}_O$-$\boldsymbol{Y}_O$ plane, and this frame rotates about $\boldsymbol{Z}_O$ in conjunction with the yaw angle ψ (Fig.3).

Now, the rotation matrix $\boldsymbol{R}_{OB}$ which expresses rotation from $\boldsymbol{B}$-frame to $\boldsymbol{O}$-frame is defined by using the basis of $\boldsymbol{B}$-frame $\boldsymbol{x}_B, \boldsymbol{y}_B, \boldsymbol{z}_B$ as follows:

$$\boldsymbol{R}_{OB} = [\boldsymbol{x}_B \quad \boldsymbol{y}_B \quad \boldsymbol{z}_B] \tag{1}$$

Similarly, $\boldsymbol{R}_{OB}$ is defined by using ϕ, θ, ψ as

$$\boldsymbol{R}_{OB} = \begin{bmatrix} c_\theta c_\psi & s_\phi s_\theta c_\psi - c_\phi s_\psi & c_\phi s_\theta c_\psi + s_\phi s_\psi \\ s_\theta s_\psi & s_\phi s_\theta s_\psi + c_\phi c_\psi & c_\phi s_\theta s_\psi - s_\phi c_\psi \\ -s_\theta & s_\phi c_\theta & c_\psi c_\theta \end{bmatrix} \tag{2}$$

Here, c_i denotes $\cos(i)$, s_i denotes $\sin(i)$, and $i = \phi, \theta, \psi$.

B. Attitude Control System

The attitude control system is designed to stabilize the attitude dynamics of the helicopter. To simplify the attitude model, we consider the following assumptions.

- Roll and pitch angle of the helicopter are sufficiently small.
- Flapping angle of the main rotor and stabilizer bar are sufficiently small.
- Yaw rate has been stabilized and almost equal to zero.

First and second assumptions are required to decouple the attitude dynamics. These assumptions could be easily satisfied in hovering or low speed situation. Third assumption is required to decouple the dynamics of angular velocity, and it could be achieved using the local feedback by rate gyro system. Under these assumptions, simple single-input single-output (SISO) state space model could be derived for roll, pitch, and yaw axis respectively. Details about the attitude model could be found in [3]. By using derived model, linear quadratic integral controller was designed for roll and pitch axis and simple PD controller was designed for yaw axis. Flight experiments have been carried out by using optical motion capture system and Inertial Measurement Unit (IMU). The results are shown in Fig.4. In these figures, solid line represents desired attitude, dashed line represents experimental result, and chain line shows simulation result by using derived model. From the figures, it is shown that the attitude of the helicopter could be stabilized and follows desired attitude. Moreover, simulation result accord with the experimental result well. Therefore, validity of derived attitude model and efficiency of designed controller was shown.

C. Guidance Control System with Collision Avoidance

In this section, guidance control system is designed by using NMPC. For the design, a mathematical model of the helicopter and a criterion used for optimization are needed. First, mathematical model of translational motion of the helicopter is derived. After applying the attitude control system to the helicopter, it could be assumed that the attitude of the helicopter immediately follows desired attitude. Therefore, the attitude dynamics could be ignored, and horizontal and vertical forces are simply considered as inputs for translational dynamics. Now, the equation of motion of the helicopter on $\boldsymbol{O}$-frame is obtained as

$$\begin{aligned} m\ddot{x} &= -k_x \dot{x}^2 + F_x \\ m\ddot{y} &= -k_y \dot{y}^2 + F_y \\ m\ddot{z} &= -k_z \dot{z}^2 + mg + F_z \end{aligned} \tag{3}$$

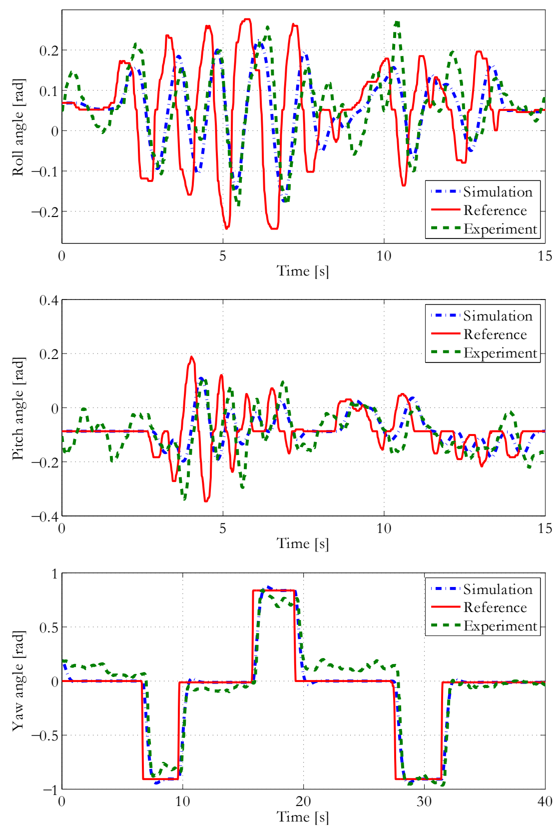

Fig. 4. Experimental result of attitude control

Here, m denotes mass of the helicopter, g is gravitational acceleration, F_x, F_y, and F_z are the external forces generated by rotor thrust, and k_x, k_y, and k_z denote coefficients relates to air resistance. Generally, k_x, k_y, and k_z are proportional to surface area of the helicopter. In hovering state, k_z could be considered as constant. However, k_x, k_y may vary in conjunction with yaw angle because the shape of helicopter is long in the anteroposterior direction (Fig.5). Therefore, k_x, k_y are considered as a function of ψ as follows:

$$k_x(\psi) = k_{xy}(l_a + l_b \sin\psi) \quad (4)$$

$$k_y(\psi) = k_{xy}(l_a + l_b \cos\psi) \quad (5)$$

Now, we consider state vector as $\boldsymbol{x} = [x\ y\ z\ \dot{x}\ \dot{y}\ \dot{z}]^T$, and input as $\boldsymbol{u} = [F_x\ \ F_y\ \ F_z\ \ \psi]^T$, then nonlinear state space equation could be obtained by using (3)-(5) as

$$\dot{\boldsymbol{x}} = \boldsymbol{f}(\boldsymbol{x}(t),\ \boldsymbol{u}(t)) \quad (6)$$

Next, criterion is derived. In this study, we adopted following criterion.

$$\begin{aligned} J &= \Phi(\bar{\boldsymbol{x}}(t+T)) \\ &+ \int_t^{t+T} \Bigg(L(\bar{\boldsymbol{x}}(\tau), \bar{\boldsymbol{u}}(\tau)) + r_u P_u(\bar{\boldsymbol{u}}(\tau)) \\ &\qquad + \frac{1}{r_x} B(\bar{\boldsymbol{x}}(\tau)) + r_c P_c(\bar{\boldsymbol{x}}(\tau)) \Bigg) d\tau \end{aligned} \quad (7)$$

Here $\bar{\boldsymbol{x}}$ and $\bar{\boldsymbol{u}}$ are estimated state and input which are predicted by using the model. First and second term of right side are terminal cost and stage cost respectively, and they are defined as follows:

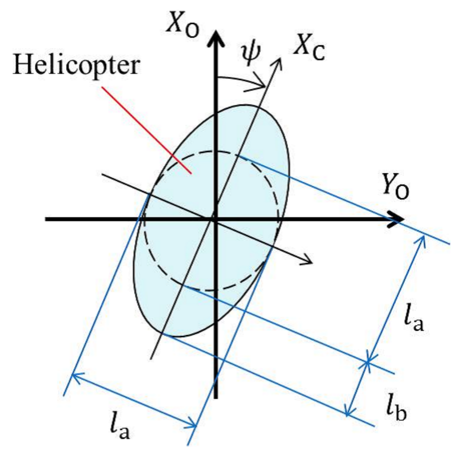

Fig. 5. Translational model

$$\Phi(\bar{\boldsymbol{x}}(t+T)) \;=\; \bar{\boldsymbol{x}}^T(t+T)\boldsymbol{S}\bar{\boldsymbol{x}}(t+T) \quad (8)$$

$$L(\bar{\boldsymbol{x}}(\tau), \bar{\boldsymbol{u}}(\tau)) \;=\; \bar{\boldsymbol{x}}^T(\tau)\boldsymbol{Q}\bar{\boldsymbol{x}}(\tau) + \bar{\boldsymbol{u}}^T(\tau)\boldsymbol{R}\bar{\boldsymbol{u}}(\tau) \quad (9)$$

Here, $\boldsymbol{S}$, $\boldsymbol{Q}$, $\boldsymbol{R}$ are weighting matrices. Third, fourth, and fifth term of right side of (7) relate to collision avoidance and input constraints. r_u, r_x, r_c are design parameters. In the following, details about constraints are described.

Third term of (7) relates to input constraints. In previous section, we assumed that the attitude of the helicopter is near hovering state. Accordingly the desired attitude angle should be limited for satisfying the assumption. We deal with such limit as an inequality constraint, and it is derived as

$$g(\bar{\boldsymbol{u}}) = \bar{F_x^i}^2 + \bar{F_y^i}^2 - (mg\sin\alpha)^2 \quad (10)$$

Here, suffix i represents i th estimate in evaluation interval, α $[rad]$ is permissible maximum tilt angle of the helicopter. The relation between the external force and the tilt angle of the helicopter is shown in Fig.6. We introduce such input constraints to criterion as the penalty function $P_u(\bar{\boldsymbol{u}}(t+\tau))$, and it could be obtained as

$$P_u(\bar{\boldsymbol{u}}) = (\max\{0, g(\bar{\boldsymbol{u}})\})^2. \quad (11)$$

Fourth and fifth term in (7) are state constraints for collision avoidance. In order to avoid the collision, the prohibited area is established around each helicopter (Fig.7). The inequality constraints could be obtained as

$$g_x(\bar{\boldsymbol{x}}) = r^2 - \left\{(\bar{x}_j^i - \bar{x}_k^i)^2 + (\bar{y}_j^i - \bar{y}_k^i)^2\right\} \quad (12)$$

Here, suffix j, k represent j th and k th helicopter, r is the radius of no entry area. To avoid the collision certainly, We introduce the constraints to criterion as the barrier function as follows:

$$B(\bar{\boldsymbol{x}}) = \frac{1}{g_x(\bar{\boldsymbol{x}})^2} \quad (13)$$

Using these constraints, collision avoidance may be

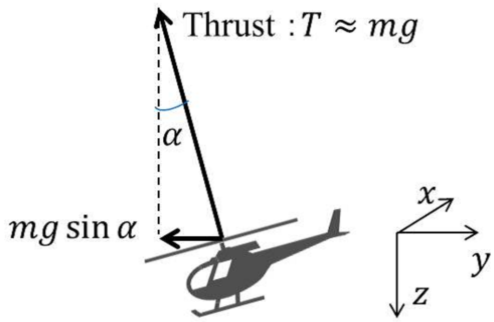

Fig. 6. Input constraint

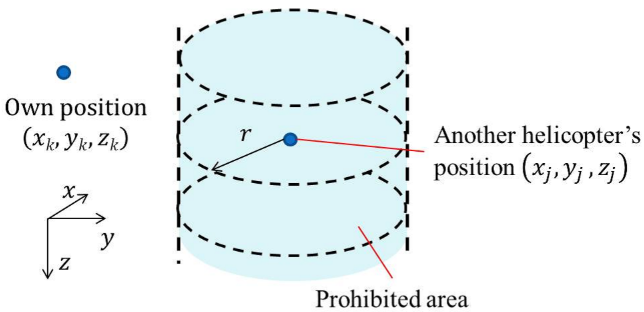

Fig. 7. Position constraint

achieved. However, the trajectory for the avoidance could not be optimized, and undesirable trajectory may be generated. For example, unnecessary detour may be caused. To fix such issue, collision avoidance method using potential function which considers a virtual obstacle to the line of the moving body is proposed. However, such potential function may have local minima. In this study, more simple method using a constraint of relative position vector of each helicopter is proposed. The constraint and penalty function are defined as follows:

$$P_c(\bar{\boldsymbol{x}}) = \begin{cases} (\max\{0, g_c(\bar{\boldsymbol{x}})\})^2, \\ if \ \ (\bar{x}_j^i - \bar{x}_k^i)^2 + (\bar{y}_j^i - \bar{y}_k^i)^2 \le (r\beta)^2 \\ and \ \ \bar{x}_{rkj}\bar{y}_{rk} - \bar{y}_{rkj}\bar{x}_{rk} > 0 \\ \\ 0, \ \ otherwise \end{cases} \tag{14}$$

$$g_c(\bar{\boldsymbol{x}}) = \bar{x}_{rkj}\bar{y}_{rk} - \bar{y}_{rkj}\bar{x}_{rk} \tag{15}$$

The definition of relative position vector is shown in Fig.8. $\bar{\boldsymbol{x}}_{rk} = [\bar{x}_{rk} \ \ \bar{y}_{rk} \ \ 0]^T$ represents the relative position vector between current position of k th helicopter and i th estimate of the position of k th helicopter in evaluation interval. $\bar{\boldsymbol{x}}_{rkj} = [\bar{x}_{rkj} \ \ \bar{y}_{rkj} \ \ 0]^T$ represents the relative position vector between the current position of k th helicopter and i th estimate of the position of j th helicopter. Using such constraint of relative position, k th helicopter could always avoid j th helicopter through the path which lies behind j the helicopter. Therefore, unnecessary detour might not be caused in avoidance process. Here, β is design parameter.

Using the model (6) and criterion (7), guidance control of

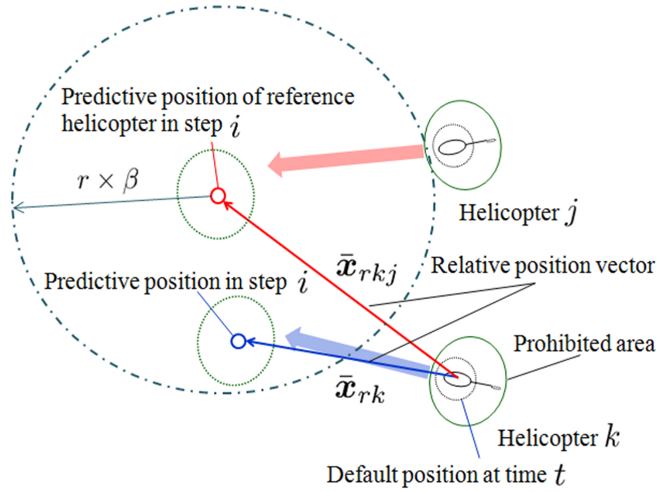

Fig. 8. Definition of relative position vector

small helicopter with collision avoidance could come down to finding optimal control to satisfy following optimization problem.

$$\begin{aligned} Minimize \ &: \ \ J \\ Subject\ to \ &: \ \ \begin{cases} \dot{\bar{\boldsymbol{x}}}(\tau) = \boldsymbol{f}(\bar{\boldsymbol{x}}(\tau), \ \bar{\boldsymbol{u}}(\tau)) \\ \bar{\boldsymbol{x}}(\tau) \mid_{\tau=0} = \boldsymbol{x}(t) \end{cases} \end{aligned} \tag{16}$$

Considering $\boldsymbol{\lambda}$ as the costate of the system, stationary condition of the optimization problem could be obtained as follows:

$$\frac{\partial \boldsymbol{x}^*}{\partial \tau} = \boldsymbol{f}(\boldsymbol{x}^*(t+\tau), \boldsymbol{u}^*(t+\tau)) \tag{17}$$

$$\boldsymbol{x}^*(\tau) \mid_{\tau=0} = \boldsymbol{x}(t) \tag{18}$$

$$\frac{\partial \boldsymbol{\lambda}^*}{\partial \tau} = -\left(\frac{\partial H}{\partial x}\right)^T (\boldsymbol{x}^*(t+\tau), \boldsymbol{u}^*(t+\tau), \boldsymbol{\lambda}^*(t+\tau)) \tag{19}$$

$$\boldsymbol{\lambda}^*(\tau) \mid_{\tau=T} = \left(\frac{\partial \Phi}{\partial x}\right)^T (\boldsymbol{x}^*(T)) \tag{20}$$

$$\frac{\partial H}{\partial \boldsymbol{u}}(\boldsymbol{x}^*(t+\tau), \boldsymbol{u}^*(t+\tau), \boldsymbol{\lambda}^*(t+\tau)) = 0 \tag{21}$$

Here, symbol $*$ means optimum solution, H denotes Hamiltonian defined by

$$H(\boldsymbol{x}, \boldsymbol{u}, \boldsymbol{\lambda}) = L(\boldsymbol{x}, \boldsymbol{u}) + r_u P_u + \frac{1}{r_x} B + r_c P_c + \boldsymbol{\lambda}^T \boldsymbol{f} \tag{22}$$

Solving (17)-(21), the optimal control series $\boldsymbol{u}^*$ could be obtained, and we use initial value of $\boldsymbol{u}^*$ for control input to the system.

Finally, the desired attitude and rotor thrust are calculated by using control input. First, the relation between the external force and the rotor thrust T_m is obtained as

$$\boldsymbol{F} = \begin{bmatrix} F_x \\ F_y \\ F_z \end{bmatrix} = \boldsymbol{R}_{OB} \begin{bmatrix} 0 \\ 0 \\ -T_m \end{bmatrix} \tag{23}$$

From the equation, T_m could be obtained as

$$T_m = ||\boldsymbol{F}|| \tag{24}$$

Next, the basis for $\boldsymbol{Z}_B$ axis on $\boldsymbol{O}$-frame could be obtained as

$$\boldsymbol{z}_B = -\frac{\boldsymbol{F}}{||\boldsymbol{F}||} \tag{25}$$

because the rotor thrust is aligned with negative direction of $\boldsymbol{Z}_B$ axis. Besides, the basis for $\boldsymbol{X}_C$ axis on $\boldsymbol{O}$-frame could be expressed by using desired yaw angle ψ_d as follows:

$$\boldsymbol{x}_C = [\cos\psi_d \ \ \sin\psi_d \ \ 0]^T \tag{26}$$

Using $\boldsymbol{z}_B$ and $\boldsymbol{x}_C$, the basis for $\boldsymbol{Y}_B$ axis and $\boldsymbol{X}_B$ axis are obtained as

$$\boldsymbol{y}_B = \frac{\boldsymbol{z}_B \times \boldsymbol{x}_C}{||\boldsymbol{z}_B \times \boldsymbol{x}_C||} \qquad \boldsymbol{x}_B = \boldsymbol{y}_B \times \boldsymbol{z}_B \tag{27}$$

Finally, the rotation matrix $\boldsymbol{R}_{OB}$ could be calculated by (1), (25), and (27). Moreover, using (2) and desired yaw angle ψ_d, desired attitude angle ϕ and θ is uniquely determined.

III. SIMULATION

Numerical simulation using designed control system was performed. In the simulation, effectiveness of designed state and input constraints were verified. In this study, we solve the two-point boundary-value problem (17)-(21) by C/GMRES method [17]. The parameters and weighting matrices used in the simulation are shown in Table I. The prediction step N is set to 20, the sampling time Δt and prediction interval $\Delta\tau$ are 0.1 [s], and prediction horizon T is $T = N \times \Delta\tau = 2$ [s].

A. Verification of input constraint

First, the input constraint was verified. In this simulation, position reference was set as step signal, and then the desired attitude generated by the guidance controller was compared in both cases which with and without the input constraint. The result is shown in Fig.9. In the figure, dashed line represents desired attitude without input constraint, solid line is with constraint, dotted line represents attitude angle which follows desired attitude with constraint. From the figure, it is clear that the desired attitude is held down to 5 [deg] in the case when there is input constraint, although large overshoot appears when there is no constraint. Moreover, the attitude angle is also suppressed below 5 deg, and the result indicates the effectiveness of the input constraint.

B. Verification of state constraint

The state constraints for collision avoidance were verified. First, collision avoidance of two helicopters was simulated. In the simulation, two helicopters fly over intersecting trajectory by using NMPC, the helicopter1 is with considering

TABLE I

SIMULATION PARAMETERS

$\boldsymbol{S}$	diag(1, 1, 1, 1, 1, 1)	$\boldsymbol{Q}$	diag(1, 1, 1, 15, 15, 15)
$\boldsymbol{R}$	diag(30, 30, 1, 10)	r_u	100
r_x	1	r_c	10
β	2	r	0.4 [m]
α	5 [deg]		

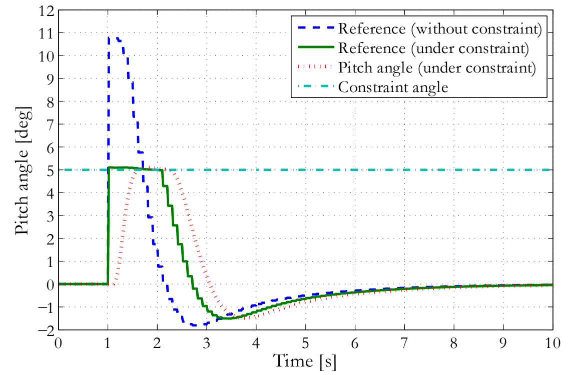

Fig. 9. Simulation result of input constraint

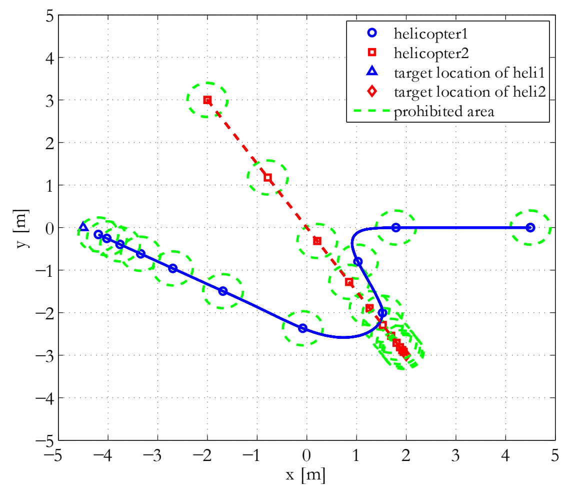

(a) Without $P_c(\bar{\boldsymbol{x}})$

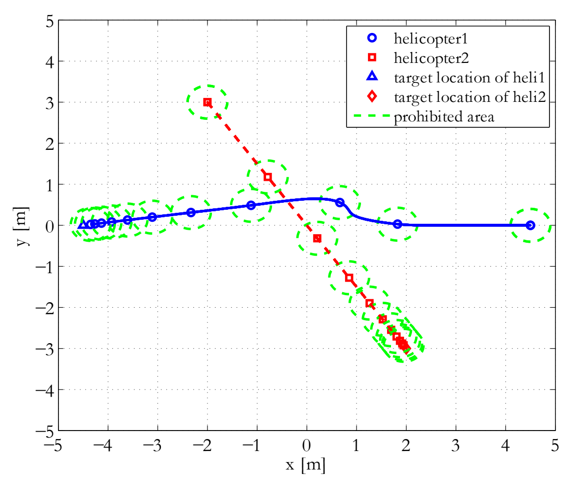

(b)With $P_c(\bar{\boldsymbol{x}})$

Fig. 10. Collision avoidance of two helicopters

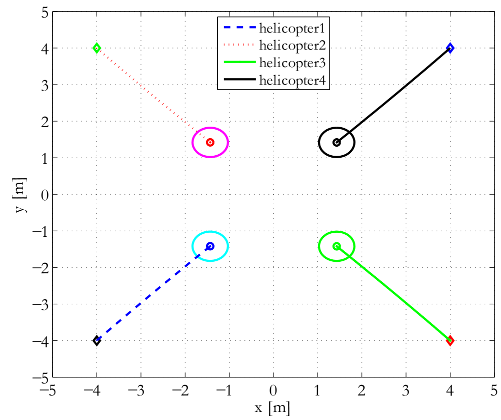

(a) $t = 3s$

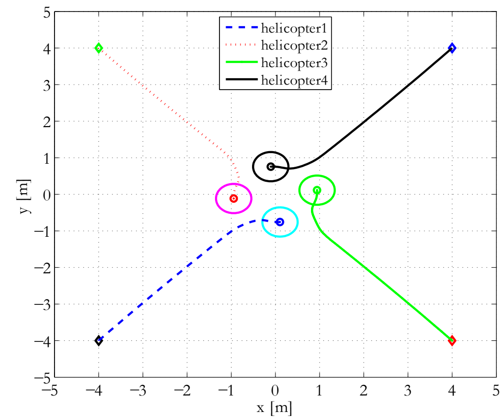

(b) $t = 8s$

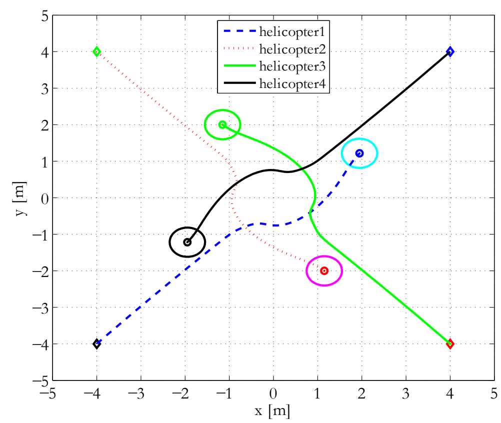

(c) $t = 12s$

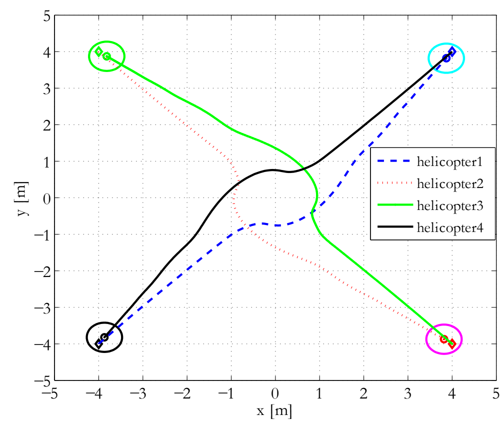

(d) $t = 30s$

Fig. 11. Collision avoidance of four helicopters

the state constraints, the helicopter2 simply goes straight to the target position. The result is shown in Fig.10. Fig.10 (a) shows the result when the constraint of relative position (14) is not considered, Fig.10 (b) shows the result with (14). From the figure, it is shown that the collision avoidance could be achieved in both cases. However, there is undesirable detour in the case when (14) is not considered because the helicopter1 crosses the path of helicopter2 at the time of the collision avoidance. By contrast, the avoidance trajectory is minimized when (14) is considered. From the results, effectiveness of the constraint of relative position is shown.

Next, the collision avoidance of four helicopters was simulated. In the simulation, four helicopters fly over intersecting trajectory, and all constraints are considered in each helicopter. In this case, the design parameter β is set to 1.5, and other parameters are same as previous simulation. The result is shown in Fig.11. From the figure, it is clear that collision-free guidance control for multiple helicopter could be achieved by proposed guidance control system.

IV. EXPERIMENT

Flight experiment was performed by using the optical motion capture system and IMU. The overview of experimental setup is shown in Fig.12.

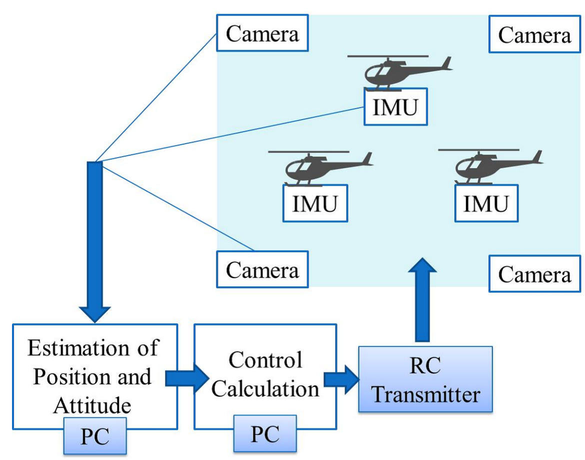

Fig. 12. Experimental setup

Guidance control experiment was carried out to verify the efficiency of designed guidance controller. In the experiment, collision avoidance for static obstacle was performed, and state constraint (12) was considered as penalty function instead of barrier function. Implementation environment and parameters for experiment are shown in Table II. Other

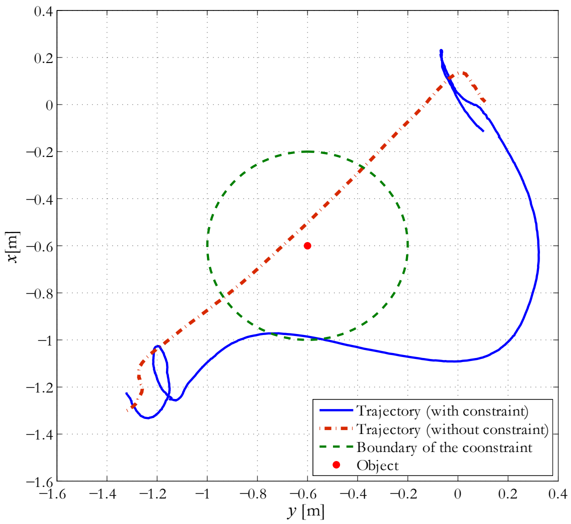

Fig. 13. Experimental result

parameters are same as which in the simulation. Then, calculation time of NMPC was 5.8 ms on the average, and it is shorter enough than the sampling time. Initial position of the helicopter was set to coordinate (-1.2 m, -1.2 m, -0.5 m) on $\boldsymbol{O}$-frame, the static obstacle was arranged on (-0.6 m, -0.6 m, 0 m). The result is shown in Fig.13. For a comparison, same control experiment was performed without state constraints for collision avoidance. In the figure, solid line represents flight trajectory of the helicopter with collision avoidance, chain line represents the trajectory without collision avoidance. From the figure, it is shown that the helicopter passed near obstacle in the case when the state constraint was not considered. In contrast, it could be verified that the helicopter avoided the obstacle and converged to the origin when the state constraint was considered. From the result, guidance controller designed in this study is available for the collision avoidance.

V. CONCLUSIONS

In this paper, we designed guidance control system for simultaneous flight of multiple small unmanned helicopter. NMPC was used for guidance controller to avoid the collision of the helicopter. The hierarchical control structure was proposed to reduce computational cost of NMPC. A novel relative position constraint was proposed for optimizing the avoidance trajectory of each helicopter. The simulation and experimental results showed the effectiveness of designed control system for collision avoidance.

In future works, simultaneous flight experiment of multiple small unmanned helicopters will be carried out.

TABLE II

ENVIRONMENT AND PARAMETER OF CONTROL

Environment	
CPU	Intel Core2 Duo
Memoly	3.45 GB
Language	C++
Parameters	
$\boldsymbol{S}$	diag(60, 60, 200, 500, 500, 10)
$\boldsymbol{Q}$	diag(20, 20, 5, 2, 2, 2)
$\boldsymbol{R}$	diag(200, 200, 200, 200)
r_x	3000
r_u	10000

REFERENCES

[1] C. K. Oh and G. J. Barlow, "Autonomous Controller Design for Unmanned Aerial Vehicles using Multi-object Genetic Programming," in *Proceedings of Congress on Evolutional Computation 2004*, vol. 2, pp. 1538-1545, 2004.

[2] J. M. Eklund, J. Sprinkle and S. Sastry, "Implementing and Testing a Nonlinear Model Predictive Tracking Controller for Aerial Pursuit/Evasion Games on a Fixed Wing Aircraft," in *Proceedings of 2005 American Control Conference*, vol. 3, pp. 1509-1514, 2005.

[3] B. Mettler, "System Identification Modeling of a Small-Scale Unmanned Rotorcraft for Flight Control Design," in *Journal of American Helicopter Society*, vol. 47, no. 1, pp. 50-63, 2002.

[4] H. J. Kim and D. H. Shim, "A Flight Control System for Aerial Robots: Algorithm and Experiment," in *Journal of Control Engineering Practice*, vol. 11, pp. 1389-1400, 2003.

[5] N. J. Eric, K. K. Suresh and K. Kannan, "Adaptive Trajectory Control for Autonomous Helicopters," in *AIAA Journal Guidance Control and Dynamics*, vol. 28, no. 3, pp. 524-538, 2005.

[6] C. L. Castillo, W. Alvis, M. Castillo-Effen, W. Moreno and K. Valavanis, "Small Unmanned Helicopter Simplified and Decentralized Optimization-based Controller Design for Non-aggressive Flights," in *International Journal on Systems Science and Applications*, vol. 1, no. 3, pp. 303-315, 2006.

[7] S. Shen, N. Michael and V. Kumar, "Autonomous Multi-floor Indoor Navigation with a Computationally Constrained MAV," in *Proceedings of IEEE International Conference on Robotics and Automation 2011*, pp. 20-25, 2011.

[8] J. H. Lee, B. M. Min and E. T. Kim, "Autopilot Design of Tilt-rotor UAV using Particle Swarm Optimization Method," in *Proceedings of the 2007 International Conference of Control, Automation and Systems*, pp. 1629-1633, 2007.

[9] H. Stone and K. C. Wong, "Preliminary Design of a Tandem-wing Tail-sitter UAV using Multi-disciplinary Design Optimization," in *Proceedings of International Aerospace Congress*, pp. 707-720, 1997.

[10] S. J. Lee, S. P. Kim, T. S. Kim, H. K. Kim and H. C. Lee, "Development of Autonomous Flight Control System for 50 m Unmanned Airship," in *Proceedings of 2004 Intelligent Sensors, Sensor Networks Information Processing Conference*, pp. 457-461, 1997.

[11] N. Michael, D. Mellinger, Q. Lindsey and V. Kumar, "The GRASP multiple micro UAV testbed," in *IEEE Robotics and Automation Magazine*, pp.56-65, 2010.

[12] D. H. Shim, H. J. Kim and S. Sastry, "Decentralized Nonlinear Model Predictive Control of Multiple Flying Robots," in *42nd IEEE CDC*, Maui, pp.3621-3626, 2003.

[13] N. Michael, J. Fink and V. Kumar "Cooperative Manipulation and Transportation with Aerial Robots," in *Autonomous Robots*, vol. 30, issue. 1, pp.73-86, 2011.

[14] F. Morteza and N. Homayoun, "An Unscented Model Predictive Control Approach to the Formation Control of Nonholonomic Mobile Robots," in *Proceedings of IEEE International Conference on Robotics and Automation 2012*, pp. 1576-1582, 2012.

[15] Y. Chai, S. Wei, M. Guo and R. Ling "Distributed Model Predictive Control with Communication Complete Failure for Multi-Aircrafts Formation ," in *Proceedings of Chinese Control and Decision Conference 2009*, pp. 4663-4668, 2009.

[16] O. Khatib, "Real-time Obstacle Avoidance for Manipulators and Mobile Robots," in *International Journal of Robotics Research*, vol.5, no.1, pp.90-98, 1986.

[17] T. Ohtsuka, "A continuation/GMRES Method for Fast Computation of Nonlinear Receding Horizon Control," in *Automatica*, vol. 40, issue. 4, pp. 563-574, 2004.